Parametric investigation of regional brain strain responses via a pre-computed atlas

Wei Zhao, Songbai Ji

Abstract We have recently established and initially validated a pre-computed brain response atlas (pcBRA) for instantaneous estimation of regional strains in contact sports. The pcBRA was created by simulating the Dartmouth Head Injury Model (DHIM) subjected to a set of pre-defined, triangulated rotational acceleration ($\boldsymbol{a}_{rot}$) impulses parameterised by the peak magnitude (a_{rot}^{p}) and duration (Δt_{rot}), as well as the azimuth (θ) and elevation (α) angles characterising the direction of rotational axis, Ω. In this study, we illustrate the potential of pcBRA for parametric studies. Specifically, by reducing the pcBRA dimensionality, we generated implicit functions in terms of color-coded surfaces and iso-contours of (i) regional average peak strains (ε_{avg}) and (ii) volume-fractions of strains above a given threshold (V_{ε}) relative to Ω for selected brain regions. For a given Ω, implicit functions of $\varepsilon_{avg}/V_{\varepsilon}$ relative to a_{rot}^{p} and Δt_{rot} as well as the resulting peak rotational velocity (v_{rot}^{p}) were also obtained. Both ε_{avg} and V_{ε} were highly dependent on Ω, and they presented non-linear relationships relative to a_{rot}^{p}, Δt_{rot} and v_{rot}^{p}. These results provide enhanced understanding of the biomechanical mechanisms of rotation-induced brain injury and may offer insight into the potential of pcBRA for future parametric or real-world applications especially in contact sports.

Keywords traumatic brain injury, pre-computation, rotation, strain, Dartmouth Head Injury Model.

I. INTRODUCTION

Traumatic brain injury (TBI) is a major public health and socioeconomic problem [1]. Indisputably, TBI induced by blunt head impact resulting from vehicular crashes, falls, assaults and contact sports is initiated through mechanical insults to the brain. Therefore, understanding the injury biomechanical mechanisms is critical for designing protective gears and for developing rules to mitigate the incidence and severity of the injury. Over the years, various injury metrics have been designed to assess TBI risks and severity. These are either defined based on linear ($\boldsymbol{a}_{lin}$; e.g. HIC [2]) or rotational ($\boldsymbol{a}_{rot}$; e.g. the rotational injury criterion (RIC), power rotational head injury criterion (PRHIC) [3] and the brain injury criterion (BrIC) [4]) acceleration alone, or on their combinations (e.g. a generalised acceleration model for brain injury threshold (GAMBIT) [5], head impact power (HIP) [6] and head impact telemetry severity profile (HITsp) [7]).

While these global kinematic variables and their variants have provided important insights into the impact scenarios associated with actual brain injuries in the real-world, they do not provide a direct correlation to region-specific, tissue-level brain mechanical responses that are thought to be directly responsible for initiating the injury [8]. To bridge the gap between external head impact and tissue-level brain responses, finite element (FE) models of the human head play an increasingly important role because of their unique capability to provide regional responses, such as strain, strain rate, stress and pressure [9]. However, these models incur a substantial computational cost (runtime and hardware) to simulate even a single head impact (typically hours or more on a modern computer or even a super-computer [10]), which poses a significant barrier to their effective deployment in real-world practical applications.

Developing a computationally efficient, yet sophisticated numerical model with high predictive power remains a major challenge [11]. Although it is conceivable to couple a high-performance computer with a simplified head model to reduce simulation runtime, degradation in solution accuracy and resolution is never desirable. This is especially true given that much more detailed and sophisticated [12] or subject-specific [13]

W. Zhao is a post-doctoral research associate in Thayer School of Engineering at Dartmouth College, USA. S. Ji is an Associate Professor of Engineering in Thayer School of Engineering, Department of Surgery, and Department of Orthopaedic Surgery at Dartmouth College, USA (tel: (603) 646-9193; fax: (603) 646-3699; e-mail: Songbai.Ji@Dartmouth.EDU).

head models are already available and continue to emerge and improve with high mesh resolution comparable to that of medical images [14] or with brain material properties incorporating structural anisotropy [15]. Consequently, computational challenges will likely persist, regardless, with a direct simulation approach.

If impact-induced brain responses can be *estimated* within seconds or instantly (vs. directly simulated in hours) without suffering from significant loss of accuracy, sophisticated head models could become much more widely adopted in a broad range of applications. This would in turn accelerate the exploration of the biomechanical mechanisms of TBI in general. The estimation scheme could also enable the establishment of injury risk metrics based on regional brain mechanical responses according to tissue-level injury tolerances, which has been envisioned before [16][17] but which has so far remained impractical due to the high demand in computation (runtime and hardware [4]). Although some loss of accuracy could occur, the substantial gain in computational efficiency, even without relying on high-end computers, appears to well justify the use of the estimation technique for real-world applications. This is especially true given that potentially even greater errors or uncertainties exist in head impact measurement, itself [18][19][20]. Further, even validated head models produce discordant model responses [21], primarily because of inconsistent characterisations of the brain material properties at present [22].

Following this line of thinking, we have recently introduced a pre-computation strategy [10] to substantially improve simulation efficiency for impacts relevant to contact sports because their temporal characteristics are largely similar [23]. Essentially, the pre-computed brain response atlas (pcBRA) establishes a high-dimensional parametric hyperspace between kinematic input and brain output responses to allow a highly efficient interpolation or extrapolation (seconds or instantaneously) without a direct simulation. The pcBRA parameterises generic, instrument-independent kinematic variables. Therefore, the atlas is anticipated to be applicable to any impact measurement system (e.g. through laboratory reconstruction [6][20], instrumented helmet [19][24], mouthguard [25][26] or anthropomorphic test device [6]), as long as input parameterisation remains feasible [10].

As the strain pcBRA samples the hyperspace regularly, it enables a convenient exploration of the causal relationships between rotational kinematic input variables and regional strain responses. The regular sampling with sufficient density also allows the generation of implicit functional forms in terms of color-coded surfaces and iso-contour curves, which were not available in previous efforts [27][28][29]. In this study, we attempt to illustrate the use of pcBRA for parametric studies by probing the relationships for generic brain regions and the corpus callosum. Findings from this study are anticipated to enhance our understanding of the mechanisms of rotation-induced TBI. Additionally, they offer important insights into the potential of pcBRA for further parametric or real-world applications especially in contact sports in the future. A subset of the spatially resampled pcBRA is freely available for research use (see Appendix) to allow further evaluation of the technique in the research community.

II. METHODS

The Dartmouth Head Injury Model (DHIM)

The pcBRA was established using our current subject-specific Dartmouth Head Injury Model (DHIM [13][30][31]; completely revamped from earlier versions; Fig. 1). The DHIM was created with high mesh quality and geometrical accuracy based on a high-resolution MRI of an actual athlete. It is composed of solid hexahedral and surface quadrilateral elements with a total of 101.4 k nodes and 115.2 k elements (56.6 k nodes and 55.1 k elements) and a combined mass of 4.562 kg (1.558 kg) for the whole head (brain). The average element size for the whole head and the brain is 3.2 ± 0.94 mm and 3.3 ± 0.79 mm, respectively. The DHIM employs a homogenous second-order Ogden hyperelastic material model with rate effects incorporated through linear viscoelasticity represented by a six-term Prony series (identical to the "average model" in [32]) to model the brain biomechanical responses. A layer of soft elements representing the cerebrospinal fluid exists between the brain and its neighboring structures (skull, falx, and tentorium) by node sharing to enable brain interfacial sliding. The DHIM has been successfully validated against relative brain-skull displacement [33][34] and intracranial pressure responses [35][36] from cadaveric experiments, as well as strain responses in a live human volunteer [37]. The overall "good" to "excellent" validation at the low (~250–300 rad/s^2 for the volunteer), mid (~1.9–2.3 krad/s^2 for impact tests C755-T2 and C383-T1), and high (~11.9 krad/s^2 for test C393-T4) levels of $\boldsymbol{a}_{rot}$ peak magnitudes provided important confidence of the accuracy of DHIM-estimated brain responses.

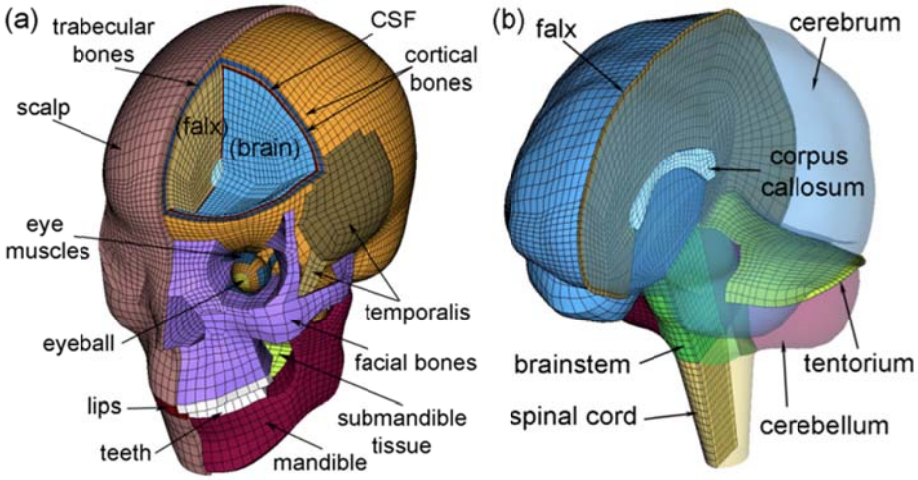

Fig. 1. The DHIM, showing color-coded head exterior (a) and intracranial components (b), which also includes part of the spinal cord to improve model biofidelity in the inferior region.

The Pre-Computed Brain Strain Response Atlas

The pcBRA was established by sampling independent rotational kinematic variables drawn from on-field measurements in helmeted contact sports using the HIT system [7]. Four independent variables of the rotational impulses were parameterised: the acceleration peak magnitude (a_{rot}^{p}) and duration (Δt_{rot}), as well as the azimuth and elevation angles (θ and α) characterising the rotational axis, Ω. Triangular rotational impulses were used. The temporal shapes of the rotational impulse were insignificant to the brain peak strain responses, as long as an identical rotational velocity and impulse duration were maintained [10]. Conceptually, this is because the converted brain strain energy is likely to be proportional to the external kinetic energy, while they are each proportional to the square of strain and square of rotational velocity, respectively. A longer duration with an identical rotational velocity lowers strain, likely because of increased strain energy dissipation due to the viscoelastic properties of the brain. As current tissue-level brain injury criteria are largely based on accumulated peak strain responses, the element-wise maximum principal strain during the entire impact simulation, regardless of the time of occurrence (ε^{p}), was used as the pcBRA reference response [10].

The ranges and sampling densities of the four variables are given in TABLE I. Due to the head geometrical symmetry relative to the mid-sagittal plane, the sampling range of Ω (θ, α) was halved (Table I; Fig. 2). In total, the pcBRA consists of 4225 (5×5×13×13) whole-brain response solutions. Because Ω degenerated to the ±z–axis when α reached ±90°, regardless of the θ values, only 3625 (4225 – 5×5×12×2) unique atlas solutions were necessary to establish the pcBRA for the given variable ranges. The pcBRA estimation accuracy was successfully verified using random sampling as well as two independently measured typical real-world resultant $\boldsymbol{\alpha}_{rot}$ profiles [10]. The estimation efficiency (6 sec or <0.01 sec for whole-brain element-wise or regional average responses, respectively) was dramatically improved over that from direct simulation (~50 min to simulate a 40 ms impulse directly using DHIM plus an additional ~5 min for post-processing).

TABLE I

SUMMARY OF THE ROTATIONAL IMPULSE PARAMETERISATION VARIABLES AND THEIR RANGES, STEP SIZES AND NUMBERS OF SAMPLES USED TO ESTABLISH THE PCBRA.

Variable	a_{rot}^{p} (rad/s^2)	Δt (ms)	θ (°)	α (°)
Range	[1500, 4500]	[4, 16]	[-90, 90]	[-90, 90]
Step size	750	3	15	15
# of samples	5	5	13	13

Data Analysis

The pcBRA essentially generated a five-dimensional (5D) grid data structure of element-wise ε^p values (a list of mesh elements plus 4D kinematic input parameters). For any regional volume-weighted average strain (ε_{avg}) and volume fraction of ε^p above a given strain threshold of 0.1 ($V_{0.1}$; strain threshold limited to 0.1 here because of the relatively mild a^p_{rot} values simulated in pcBRA), the grid data structure was reduced to 4D. To visualise the implicit functional forms of ε_{avg} and V_ε relative to the rotational kinematic variables, further reduction in dimensionality was necessary. This was achieved by fixing a^p_{rot} and Δt_{rot} to 4.5 krad/s^2 and 10 ms, respectively, to visualise the relationship relative to the rotational axis, Ω; or by fixing Ω to a coronal rotation (i.e. θ = 0° and α = 0°), to visualise the relationship relative to a^p_{rot} and Δt_{rot}. For both ε_{avg} and $V_{0.1}$, generic brain regions (whole brain, cerebrum, cerebellum, brainstem) and a targeted region (corpus callosum) were considered. The anatomical boundary of corpus callosum was determined from segmentation using FreeSurfer software package (version 5.1). To improve visualisation resolution, brain responses at a more refined sampling density were interpolated (5° for θ and α, 60 rad/s^2 and 0.2 ms for a^p_{rot} and Δt_{rot}, respectively), which remained sufficiently accurate [10]. All data analyses were performed in Matlab 2014a.

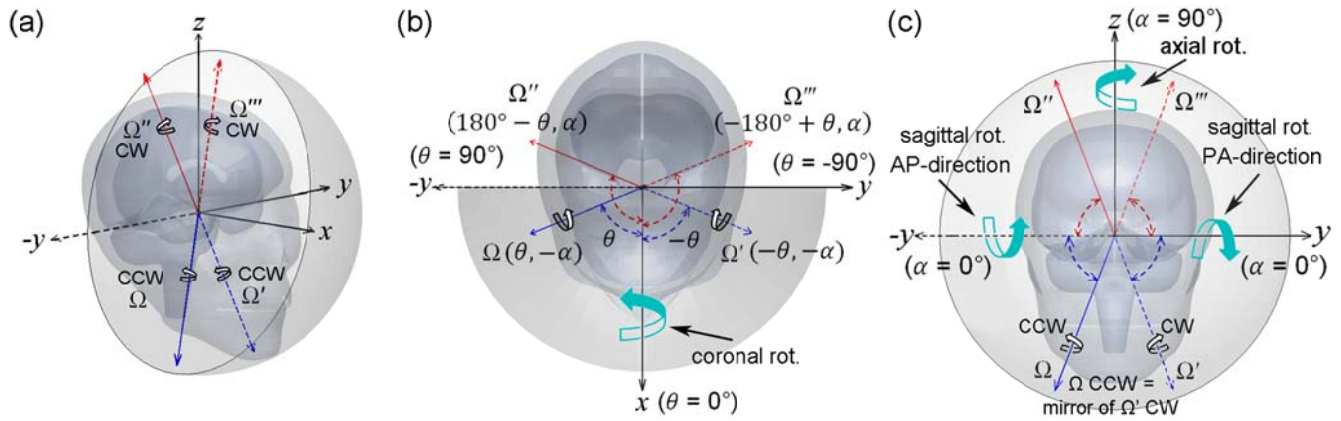

Fig. 2. Schematic of head rotational axes and the sampling space in iso- (a), top (b), and frontal (c) views. Brain strain responses generated by Ω and Ω'' (solid), or by Ω' and Ω''' (dashed) are symmetric about the mid-sagittal plane (*xz*-plane; all counter-clockwise (CCW) rotations). A CCW rotation about Ω generates a symmetric response relative to that from a clockwise (CW) rotation about Ω'. The shaded hemisphere represents the pcBRA sampling space for Ω (i.e. both θ and α range [-90°, 90°]).

III. RESULTS

Fig. 3(a) illustrates ε_{avg} for the corpus callosum as an implicit function relative to Ω CCW rotation (Fig. 3(b)). Similarly to Fig. 2, each point on the hemispherical surface represents the end-point of a given Ω with color-coded ε_{avg}. The largest ε_{avg} occurred when θ and α were both 15°, near a coronal rotation. For any Ω CCW rotation, the mirroring axis, Ω', with CW rotation (Fig. 3(e)), produced a mirroring response relative to the mid-sagittal plane (Fig. 3(c) and (f)). Consequently, for any geometrically symmetric region of interest (ROI), the ε_{avg} value corresponding to Ω' CW rotation was identical to that from Ω CCW rotation (Fig. 3(a) and (d)). For the remainder of the results, therefore, the implicit functions for other geometrically symmetric regions are only shown for the sampling space corresponding to Ω CCW rotation to avoid repetition.

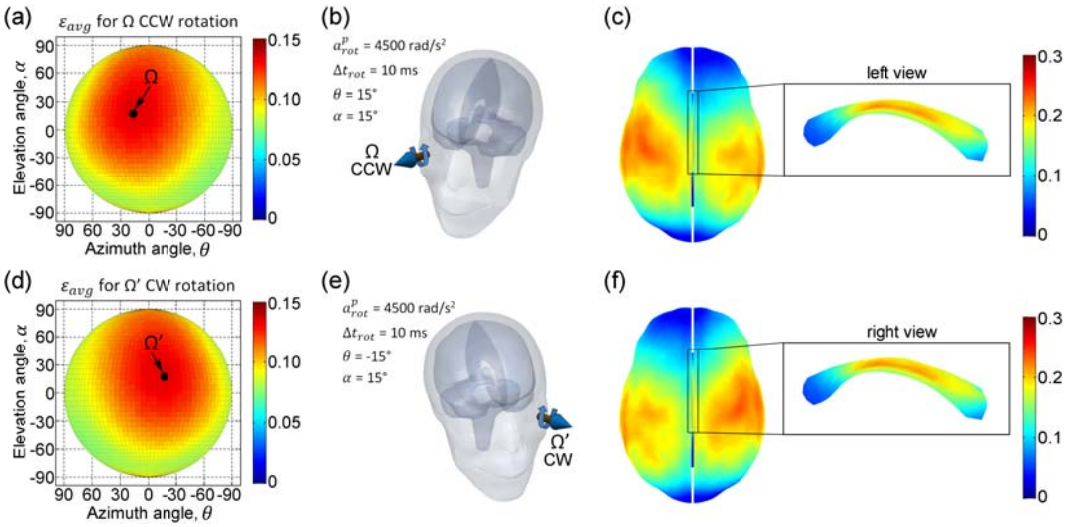

Fig. 3. The implicit function of ε_{avg} for the corpus callosum corresponding to the counter-clockwise (CCW) rotations about Ω (a) and the clockwise (CW) rotations about Ω' (d). A CCW rotation about Ω in the chosen sampling space (b) and a CW rotation about Ω' in the mirroring sampling space (e) produced mirroring $\boldsymbol{\varepsilon^p}$ distributions ((c) and (f)), resulting in an identical $\boldsymbol{\varepsilon_{avg}}$ for any geometrically symmetric ROI.

The implicit functions of regional ε_{avg} relative to the rotational axis are shown in Fig. 4 for the selected brain ROIs for the same given a^p_{rot} and Δt_{rot}. Their corresponding $V_{0.1}$ are presented in Fig. 5.

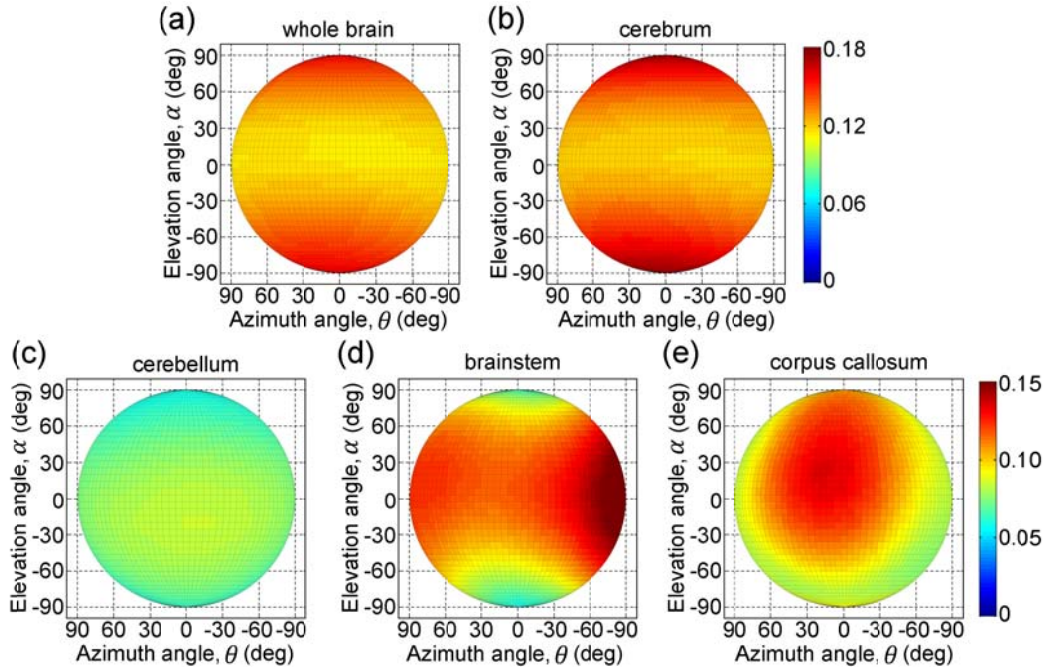

Fig. 4. Implicit functions of ε_{avg} relative to the θ and α angles characterising Ω in selected ROIs for the given a^p_{rot} (4.5 krad/s^2) and Δt_{rot} (10 ms). Note the different color bar scales in the top and bottom rows.

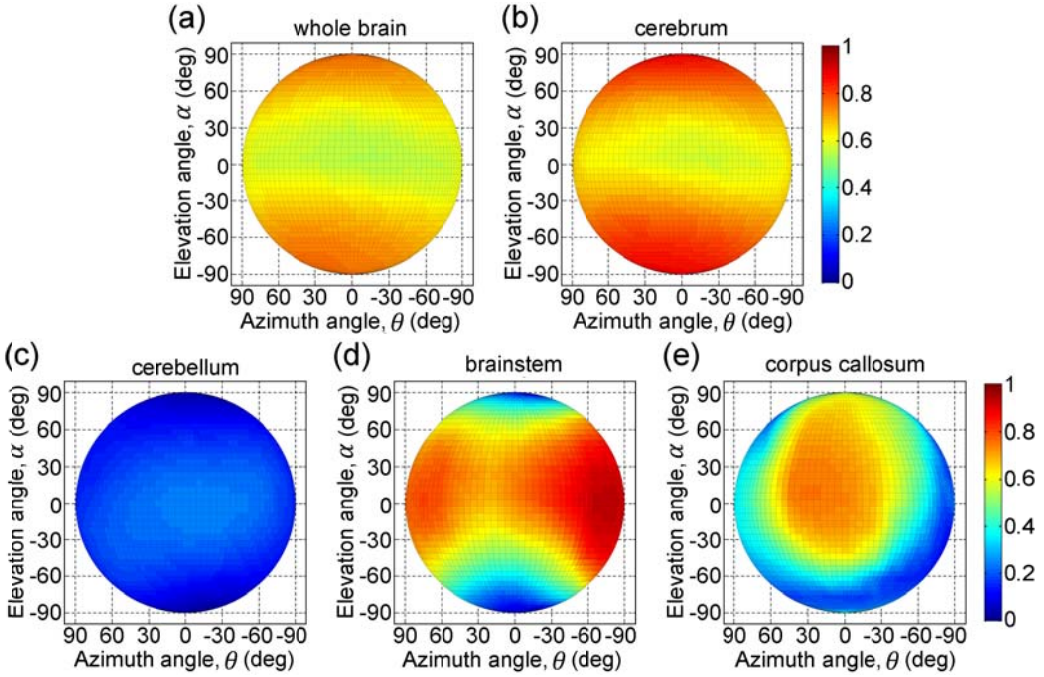

Fig. 5. Implicit functions of $V_{0.1}$ relative to θ and α angles characterising Ω in selected ROIs for the given a_{rot}^{p} (4.5 krad/s^2) and Δt_{rot} (10 ms).

For a given coronal rotation (i.e. θ = 0° and α = 0°), ε_{avg} and $V_{0.1}$ in each ROI formed a non-linear relationship relative to a_{rot}^{p} and Δt_{rot}, as highlighted by the iso-contours (Fig. 6 and Fig. 7). The a_{rot}^{p} and Δt_{rot} influenced both ε_{avg} and $V_{0.1}$ interactively. Both responses increased with either a_{rot}^{p} or Δt_{rot} when the other was fixed.

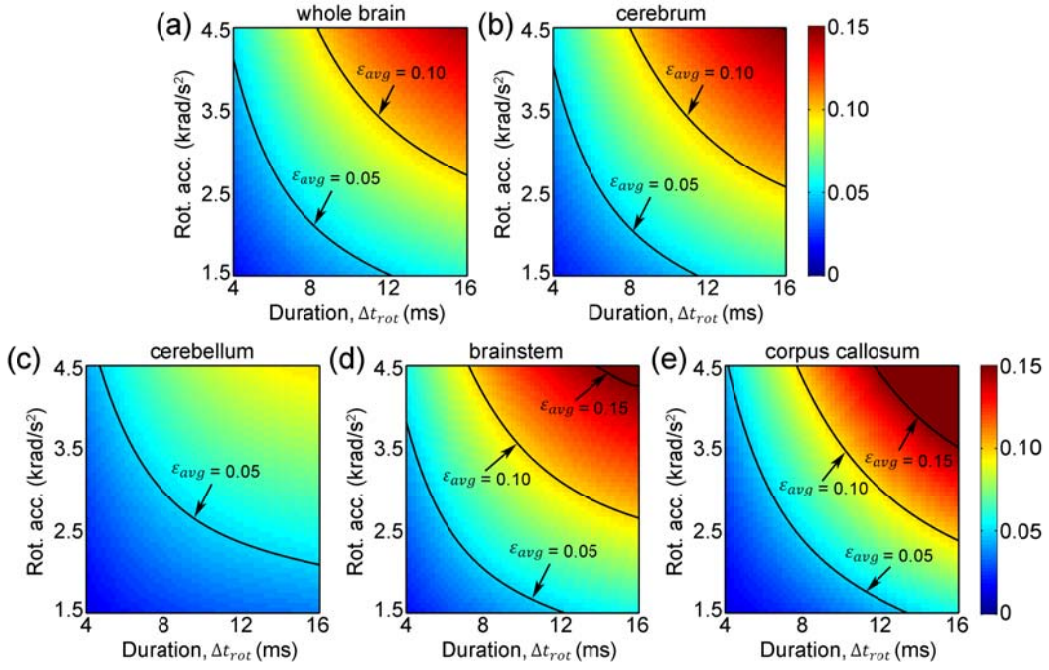

Fig. 6. Implicit functions of ε_{avg} relative to a_{rot}^{p} and Δt_{rot} for the given Ω (θ = 0°, α = 0°; coronal rotation). Iso-contours at selected ε_{avg} levels are also shown.

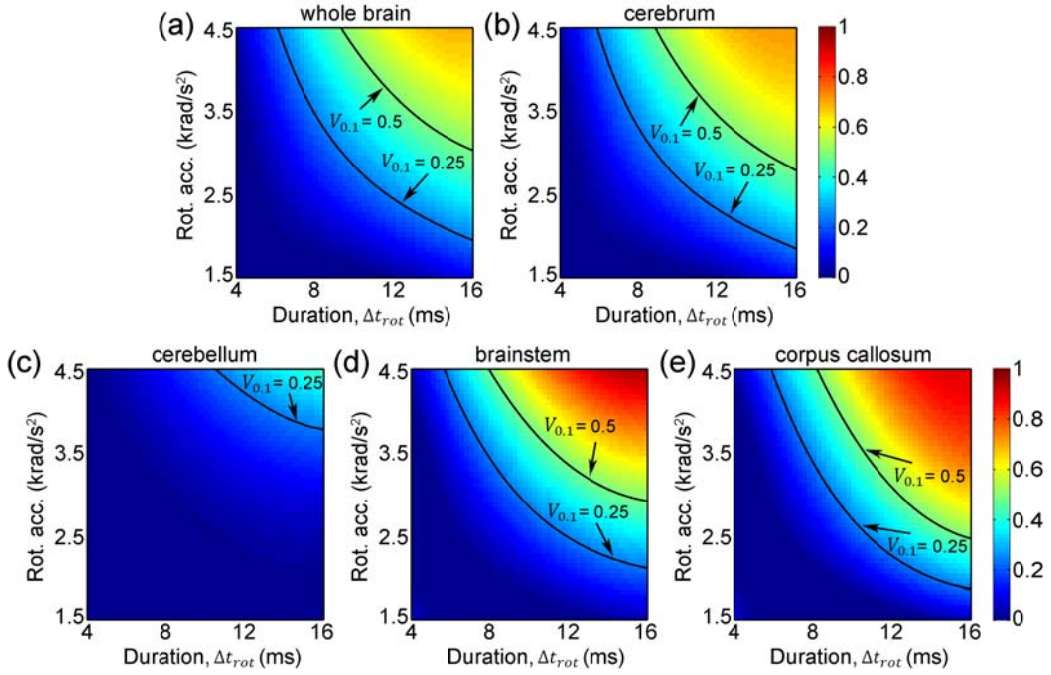

Fig. 7. Implicit functions of $V_{0.1}$ relative to a_{rot}^{p} and Δt_{rot} for the given Ω (θ = 0°, α = 0°; coronal rotation), with iso-contours at selected $V_{0.1}$ levels.

The implicit functions of ε_{avg} and $V_{0.1}$ relative to v_{rot}^{p} were obtained by multiplying a_{rot}^{p} and Δt_{rot}. As the brain strain pcBRA directly sampled a_{rot}^{p} but not v_{rot}^{p}, only a subset of regular grid structure was available for the combination of v_{rot}^{p} and Δt_{rot} (Fig. 8 and Fig. 9). In general, both ε_{avg} and $V_{0.1}$ increased with the increase of v_{rot}^{p} for a given Δt_{rot}, while they slightly decreased with the increase of Δt_{rot} for an identical v_{rot}^{p} (Fig. 8 and Fig. 9).

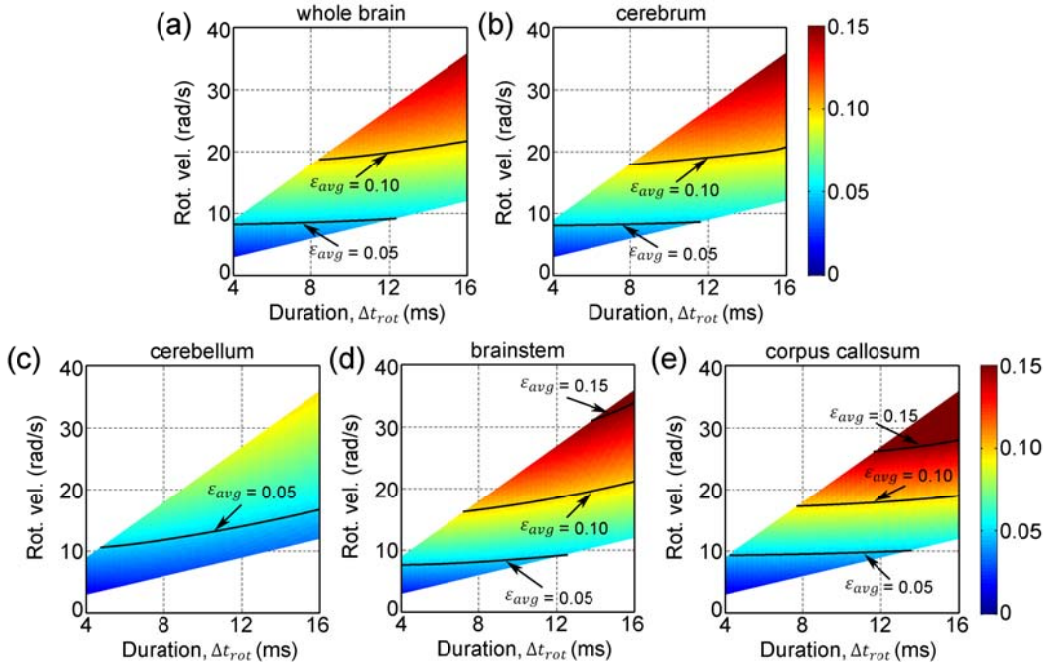

Fig. 8. Implicit functions of ε_{avg} relative to v_{rot}^{p} and Δt_{rot} for the given Ω (θ = 0°, α = 0°; coronal rotation), with iso-contours at selected levels. The parametric space appears incomplete because the pcBRA directly samples a_{rot}^{p} and Δt_{rot} but not v_{rot}^{p} and Δt_{rot}.

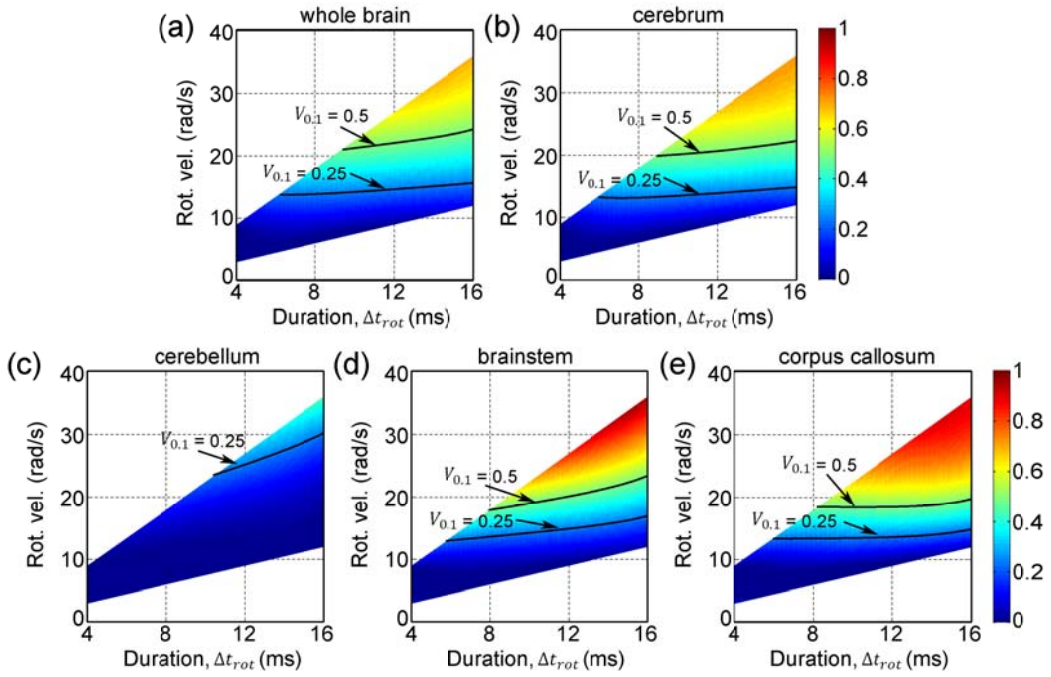

Fig. 9. Implicit functions of $V_{0.1}$ relative to v_{rot}^{p} and Δt_{rot} for the given Ω (θ = 0°, α = 0°; coronal rotation), with iso-contours at selected levels.

IV. DISCUSSION

Understanding the causal relationship between head kinematic input and regional brain responses is important to ultimately elucidate the biomechanical mechanisms of TBI. An enhanced understanding may also allow future brain injury metrics to be designed based on tissue-level mechanical responses in targeted regions rather than on global kinematic variables or their variants alone. For a given head FE model, such a kinematic input vs. response output relationship is essentially a high-dimensional functional mapping between independent input variables and tissue-level mechanical response parameters. The pcBRA samples the parametric hyperspace into a regular grid data structure, which allows rapid and convenient exploration of the hyperspace. As an illustration, the current study represents our initial attempt to probe the causal relationships for generic ROIs and the corpus callosum. To reduce the pcBRA dimensionality for visualisation, implicit functions were generated at selected a_{rot}^{p} and Δt_{rot} values (4.5 krad/s^2 and 10 ms, respectively) for the rotational axis, Ω, as well as at a selected Ω (θ = 0° and α = 0°, i.e. coronal rotation) for a_{rot}^{p} and Δt_{rot}.

Significant directional dependency was evident for most regional brain responses, consistent with findings from previous model-based [27,28,38] and animal injury studies [39–41]. For the given a_{rot}^{p} and Δt_{rot} values, both regional brain average peak strains (ε_{avg}) and the volume fractions above a given strain threshold of 0.1 ($V_{0.1}$) strongly depended on the direction of Ω and were region-specific (Fig. 4 and Fig. 5). For the whole-brain and cerebrum, an axial rotation (α = ±90°) produced the largest ε_{avg} and $V_{0.1}$, consistent with an earlier report [27] and recent FE studies [4][42]. For example, the critical $\boldsymbol{v}_{rot}^{p}$ value of BrIC for axial rotation (i.e. α of 90° or -90°, or the "north" or "south" pole in Fig. 5) was found to be the lowest for a given V_{ε} (20–40% lower than that for coronal or sagittal rotations based on V_{ε} or strain responses) [4]. Similarly, the critical $\boldsymbol{v}_{rot}^{p}$ value for axial rotation was reported to be 30–40% lower than that for the other two rotations using strain responses with the latest KTH model [42]. Conversely, these reports suggest the largest whole-brain V_{ε} or ε_{avg} occur when rotating in an axial plane for a given $\boldsymbol{v}_{rot}^{p}$, as reported here.

Interestingly, the axial rotation led to the lowest responses for the brainstem, whose largest response occurred in a sagittal rotation instead, corresponding to an occipital impact (i.e. θ = -90° and α = 0°). This agreed with findings from the SIMon [27], but differed from that in another study reporting a coronal rotation to result in the largest strain in the brainstem [28]. These findings also appeared inconsistent with the reports on monkeys [39], where no brainstem injury occurred in sagittal rotations. For the cerebellum, the directional dependency was less evident with a more uniform distribution across the spectrum of Ω, likely due to its relatively tight anatomical confinement. However, this was inconsistent with an earlier report that instead

found significant V_ε values with a 45° oblique rotation (θ = 0°, α = -45°) [27]. Notably, the cerebellum also had a much smaller strain response regardless of Ω (Fig. 4 and Fig. 5), which agreed well with clinical findings that direct cerebellar injury is relatively uncommon [43].

In contrast, the corpus callosum had the largest ε_{avg} when θ and α were both 15° (Fig. 3), corresponding to a slightly oblique coronal rotation (largely confirming previous report [28]). This agreed well with previous neuropathological observations on monkeys, where the coronally injured monkeys sustained most severe axonal damages in the corpus callosum [39]. Because these selected generic or targeted ROIs were symmetrical relative to the mid-sagittal plane, either the CCW or CW axial rotations (i.e. the "north" or "south" poles in Fig. 4 and Fig. 5, respectively) led to identical ε_{avg} or V_ε responses (confirmed, including the corpus callosum).

For a given Ω (θ = 0° and α = 0°, i.e. coronal rotation), the input-output implicit functions were non-linear in each ROI. As anticipated, larger a_{rot}^p with an identical Δt_{rot} led to larger ε_{avg} for all brain regions. This was similarly observed in previous physical models, where maximum shear strain (vs. maximum principal strain here) increased with the increase of a_{rot}^p at a given location (vs. regional average) [44,45]. It was intriguing that the iso-contours of ε_{avg} and $V_{0.1}$ (Fig. 6 and Fig. 7) were similar in shape compared to the well-known tolerance curve for a_{rot}^p and Δt_{rot} established based on concussed and non-concussed monkeys [46] (albeit our data was confined to much lower a_{rot}^p values, even after compensating for geometrical scaling). Both a smaller a_{rot}^p but larger Δt_{rot} or, conversely, a larger a_{rot}^p but smaller Δt_{rot}, could result in an identical ε_{avg} or $V_{0.1}$. This highlighted the importance of both a_{rot}^p and Δt_{rot} in strain or its resulting TBI risk, consistent with a recent animal study using rats that quantified rotation-induced injury with cognitive metrics and diffusion tensor imaging parameters [47]. Collectively, these findings suggest that injury risk metrics based on both a_{rot}^p and Δt_{rot} may be more effective than those relying on a_{rot}^p alone [48][49][50].

The implicit functions of ε_{avg} and $V_{0.1}$ relative to a_{rot}^p and Δt_{rot} were similarly region-specific. For a given coronal rotation (θ = 0°, α = 0°), it appeared that more localised regions, such as the brainstem and corpus callosum, were more sensitive to the increase of a_{rot}^p and Δt_{rot} than other ROIs (Fig. 6 and Fig. 7). Interestingly, the iso-contours of ε_{avg} and $V_{0.1}$ relative to rotational velocity, v_{rot}^p, and Δt_{rot} (Fig. 8 and Fig. 9), were much less variable, suggesting that v_{rot}^p is a more relevant kinematic indicator for regional strain responses than a_{rot}^p alone [4] [30][32] [51]. These findings were consistent with the notion of the importance of Δt_{rot}. However, for a given v_{rot}^p, increasing Δt_{rot} lowered regional brain strain responses [28], especially at higher response magnitudes (Fig. 8 and Fig. 9). This was likely a consequence of increased dissipation of brain strain energy, with a longer impulse duration due to brain's viscoelastic properties [10]. Therefore, even with an identical v_{rot}^p kinematic input, it appears that increasing the impulse duration may still mitigate strain-induced injury risks to some degree.

The current study represents our initial attempt to probe the causal relationships between rotational kinematic variables and regional brain strain responses using the recently established pcBRA. The same technique can be readily applied to other, more targeted regions, such as the mid-brain, white matter or, in fact, any arbitrary brain region. Perhaps of particular interest is the relationship for white matter fiber-oriented strains because several recent studies [13][42][52][53] have suggested the importance of incorporating white matter structural anisotropy in mTBI [54]. As the geometrical symmetry may no longer exist, a complete sampling space, including both Ω CCW rotation and Ω' CW rotation, would be needed to capture the entire Ω parametric space in this case.

It must be recognised that results reported here should be interpreted within the context of pcBRA-inherited limitations. Most notably, the pcBRA was designed and intended for use in contact sports where the temporal characteristics of head impacts appear largely similar (i.e., one major impulse dominates with additional much smaller secondary peaks [25][55]). The pcBRA parameterises the single largest rotational acceleration peak but does not yet consider the potentially significant influence from secondary deceleration peaks that inevitably follow in real-world impacts or possible varying rotational axis during impact [10]. Therefore, results from this study were effectively a first-order approximation. The same limitation also applies to previous studies that similarly employed idealised profiles (e.g. acceleration-only [27][28]; symmetric rotational velocity profiles that led to equal magnitude and duration of acceleration and deceleration [4]).

While results from the pcBRA in its current form (i.e., parameterised triangular rotational impulses corresponding to the largest single peak in $\boldsymbol{a}_{rot}$) cannot be simply extended to other, more complex head

rotations, it appears that the pcBRA-estimated strain may, regardless, still be able to provide certain limited guidance to that from the direct simulation (e.g., a bound to the directly simulated strain level). Such ability appears desirable and may be an important step forward, considering the ubiquitous application and report of the $\boldsymbol{a}_{rot}$ peak magnitude that is known to be inconsequential to brain strains (instead, rotational velocity is more strain-relevant, as demonstrated in Fig. 8 and Fig. 9). Although more sophisticated, kinematics-based injury criteria such as RIC, PRHIC [3] and BrIC [4] explicitly include rotational velocity, they do not directly provide brain strain responses either. Further, it is also important to note that the accuracy (and even "validity" in some extreme cases) of the directly simulated brain strain responses using "realistic" (vs. parameterised) head impacts may also be subject to interpretation, because of the seemingly unavoidable errors in impact measurement [18][19][20] and uncertainties in model assumptions (material properties in particular [22]). Given the current practical challenges in model-based brain injury studies in the field as discussed recently [13], the pcBRA technique seems to open a new avenue unexplored before and appears well worth pursuing.

On the other hand, it may be possible to further improve the pcBRA accuracy by incorporating second-order influences from additional $\boldsymbol{a}_{rot}$ peaks that are conceivably similar in temporal characteristics as well in contact sports. If it is feasible to probe their causal influences on brain strain responses, for example, via pattern recognition of the $\boldsymbol{a}_{rot}$ temporal profiles and machine learning techniques, compensation for response perturbation may be possible; thereby improving the accuracy compared with that from direct simulation. Obviously, this requires temporally validated on-field rotational acceleration profiles, which appear yet to be developed [18]. Despite all these accuracy concerns, it awaits further exploration whether the pcBRA-estimated strains could aid other kinematics-based, empirically derived injury criteria in discriminating injury vs. non-injury. None of them incorporates the full $\boldsymbol{a}_{rot}$ history at present.

Nevertheless, an additional limitation of our study was that the range of a_{rot}^{p} evaluated was limited [10] and did not sample higher a_{rot}^{p} impacts that are likely more injury-relevant [24][56]. However, we expect similar implicit functions to follow because the parametric hyperspace appears and is anticipated to be smooth and continuous. Further, expanding the pcBRA sampling ranges and repeating the implicit functional mapping are straightforward.

Despite these limitations and concerns, our investigation significantly extended previous studies [27–29] by providing implicit functions to directly characterise the input-response causal relationships, which were not available before. The implicit functions can also be fit into appropriate mathematical models to characterise the functional mappings (e.g. iso-contours in Figs 6–9 while further accounting for Ω). The resulting explicit, analytical forms could allow much more complete navigation of the parametric hyperspace, which was limited in the current study. However, it warrants additional investigation into whether and how these forms could be useful in the future.

V. CONCLUSIONS

Using the DHIM-based pcBRA, we have investigated the causal relationships between rotational kinematic inputs and regional brain strain responses in terms of implicit functions. The regional strains were highly dependent on the direction of rotation and were region-specific. For the whole-brain, our study largely confirmed previous reports. However, differences were observed in more localised regions, such as the cerebellum, brainstem and corpus callosum, suggesting model differences exist. The non-linear functions of strain responses relative to rotational acceleration highlight the importance of both acceleration magnitude and duration in strain. These findings enhance our understanding of brain biomechanics and may offer insight into the potential of pcBRA for parametric or real-world applications especially in contact sports in the future.

VI. ACKNOWLEDGEMENT

This work was sponsored, in part, by the NIH Grants R01NS092853, R21 NS088781 and R21 NS078607, and the Dartmouth Hitchcock Foundation.

VII. APPENDIX

A subset of the strain pcBRA was spatially resampled and is freely available, along with associated analysis software for research use and evaluation, at http://www.thayer.dartmouth.edu/~songbai_ji/DHIM/.

VIII. REFERENCES

[1] CDC. Report to Congress on Traumatic Brain Injury in the United States : Understanding the Public Health Problem among Current and Former Military Personnel, USA, June 2013.

[2] Versace, J. A review of the severity index. *15th Stapp Car Crash Conference*, 1971, Coronado, CA (USA), SAE paper No. 710881.

[3] Kimpara, H., and Iwamoto, M. Mild traumatic brain injury predictors based on angular accelerations during impacts. *Ann. Biomed. Eng*., 2012, 40(1): 114–26.

[4] Takhounts, E. G., Craig, M. J., Moorhouse, K., McFadden, J., and Hasija, V. Development of Brain Injury Criteria (BrIC). *Stapp Car Crash J.*, 2013, 57: 243–66.

[5] Newman, J. A generalized acceleration model for brain injury threshold (GAMBIT). *Proceedings of IRCOBI Conference*, 1986:121–131, Zurich (Switzerland)

[6] Newman, J., and Shewchenko, N. A proposed new biomechanical head injury assessment function-the maximum power index. *Stapp Car Crash J.*, 2000, 44(724): 215–247.

[7] Greenwald, R., Gwin, J., Chu, J., and Crisco, J. Head impact severity measures for evaluating mild traumatic brain injury risk exposure. *Neurosurgery*, 2008, 62(4): 789–798.

[8] Morrison III, B., Cullen, D., and LaPlaca, M. In vitro models for biomechanical studies of neural tissues. *Neural Tissue Biomech. Stud. Mechanobiol. Tissue Eng. Biomater.*, 2011, 3:247–285.

[9] Yang, K., Mao, H., Wagner, C., Zhu, F., Chou, C. C., and King, A. I. Modeling of the Brain for Injury Prevention. *Neural Tissue Biomechanics: Studies in Mechanobiology, Tissue Engineering and Biomaterials*, pages 69–120, *Springer-Verlag*, Berlin Heidelberg, 2011.

[10] Ji, S., and Zhao, W. A pre-computed brain response atlas for instantaneous strain estimation in contact sports. *Ann. Biomed. Eng.*, 2014. (In press)

[11] Goriely, A., Geers, M. G. D., Holzapfel, G. A., Jayamohan, J., Jérusalem, A., Sivaloganathan, S., Squier, W., Dommelen, J. A. W. Van, Waters, S., and Kuhl, E. Mechanics of the brain: perspectives , challenges , and opportunities. *Biomech. Model. Mechanobiol.*, 2015. (In press)

[12] Zhang, L., Yang, K. H., Dwarampudi, R., Omori, K., Li, T., Chang, K., Hardy, W. N., Khalil, T. B., and King, a I. Recent advances in brain injury research: a new human head model development and validation. *Stapp Car Crash J.*, 2001, 45: 369–94.

[13] Ji, S., Zhao, W., Ford, J. C., Beckwith, J. G., Bolander, R. P., Greenwald, R. M., Flashman, L. A., Paulsen, K. D., and McAllister, T. W. Group-wise evaluation and comparison of white matter fiber strain and maximum principal strain in sports-related concussion. *J. Neurotrauma*, 2015, 32(7): 441–454.

[14] Chen, Y., and Ostoja-Starzewski, M. MRI-based finite element modeling of head trauma: spherically focusing shear waves. Acta *Mech.*, 2010, 213(1-2): 155–167.

[15] Giordano, C., and Kleiven, S. Connecting fractional anisotropy from medical images with mechanical anisotropy of a hyperviscoelastic fibre-reinforced constitutive model for brain tissue. *J. R. Soc. Interface*, 2014, 11: 1–14.

[16] Franklyn, M., Fildes, B., Zhang, L., Yang, K., and Sparke, L. Analysis of finite element models for head injury investigation: reconstruction of four real-world impacts. *Stapp Car Crash J.*, 49, 2005:1–32.

[17] Ward, C., Chan, M., and Nahum, A. Intracranial Pressure-A Brain Injury Criterion. SAE Technical Paper, No. 801304, 1980

[18] Allison, M. a, Kang, Y. S., Bolte, J. H., Maltese, M. R., and Arbogast, K. B. Validation of a helmet-based system to measure head impact biomechanics in ice hockey. *Med. Sci. Sports Exerc.*, 2014, 46(1): 115–23.

[19] Beckwith, J. G., Greenwald, R. M., and Chu, J. J. Measuring head kinematics in football: correlation between the head impact telemetry system and Hybrid III headform. *Ann. Biomed. Eng.*, 2012, 40(1):237–48.

[20] Newman, J. A., Beusenberg, M. C., Shewchenko, N., Withnall, C., and Fournier, E. Verification of biomechanical methods employed in a comprehensive study of mild traumatic brain injury and the effectiveness of American football helmets. *J. Biomech.*, 2005, 38(7):1469–81.

[21] Ji, S., Ghadyani, H., Bolander, R. P., Beckwith, J. G., Ford, J. C., McAllister, T. W., Flashman, L. A, Paulsen, K. D., Ernstrom, K., Jain, S., Raman, R., Zhang, L., and Greenwald, R. M. Parametric Comparisons of Intracranial Mechanical Responses from Three Validated Finite Element Models of the Human Head. *Ann. Biomed. Eng.*, 2014, 42(1): 11–24.

[22] Chatelin, S., Constantinesco, A., and Willinger, R. Fifty years of brain tissue mechanical testing : From in vitro to in vivo investigations. *Biorheology*, 2012, 47(5–6):255–276.

[23] Broglio, S. P., Schnebel, B., Sosnoff, J. J., Shin, S., Fend, X., He, X., and Zimmerman, J. Biomechanical properties of concussions in high school football. *Med. Sci. Sports Exerc.*, 2010, 42(11): 2064–71.

[24] Rowson, S., Brolinson, G., Goforth, M., Dietter, D., and Duma, S. Linear and angular head acceleration measurements in collegiate football. *J. Biomech. Eng.*, 2009, 131(6): No. 061016.

[25] Camarillo, D. B., Shull, P. B., Mattson, J., Shultz, R., and Garza, D. An instrumented mouthguard for measuring linear and angular head impact kinematics in American football. Ann. Biomed. Eng., 2013, 41(9): 1939–49.

[26] Bartsch, A., Samorezov, S., Benzel, E., Miele, V., and Brett, D. Validation of an "Intelligent Mouthguard" single event head impact dosimeter. *Stapp Car Crash J.*, 2014, 58:1–28.

[27] Weaver, A. A., Danelson, K. A., and Stitzel, J. D. Modeling brain injury response for rotational velocities of varying directions and magnitudes. *Ann. Biomed. Eng.*, 2012, 40(9): 2005–18.

[28] Kleiven, S. Evaluation of head injury criteria using a finite element model validated against experiments on localized brain motion, intracerebral acceleration, and intracranial pressure. *Int. J. Crashworthiness*, 2006, 11(1): 65–79.

[29] Zhou, C., Khalil, T., and King, A. Viscoelastic response of the human brain to sagittal and lateral rotational acceleration by finite element analysis. *Proceedings of IRCOBI Conference*, 1997: 35–48, Dublin (Ireland).

[30] Ji, S., Zhao, W., Li, Z., and McAllister, T. W. Head impact accelerations for brain strain-related responses in contact sports: a model-based investigation. *Biomech. Model. Mechanobiol.*, 2014, 13(5):1121–36.

[31] Zhao, W., Ruan, S., and Ji, S. Brain pressure responses in translational head impact: a dimensional analysis and a further computational study. *Biomech. Model. Mechanobiol.* 2014, (In press).

[32] Kleiven, S. Predictors for Traumatic Brain Injuries Evaluated through Accident Reconstructions. *Stapp Car Crash J.*, 2007, 51: 81–114.

[33] Hardy, W. N., Mason, M. J., Foster, C. D., Shah, C. S., Kopacz, J. M., Yang, K. H., King, A. I., Bishop, J., Bey, M., Anderst, W., and Tashman, S. A Study of the Response of the Human Cadaver Head to Impact. *Stapp Car Crash J.*, 2007, 51:17–80.

[34] Hardy, W. N., Foster, C. D., Mason, M. J., Yang, K. H., King, a I., and Tashman, S. Investigation of Head Injury Mechanisms Using Neutral Density Technology and High-Speed Biplanar X-ray. *Stapp Car Crash J.*, 2001, 45: 337–68.

[35] Nahum, A., Smith, R., and Ward, C. Intracranial pressure dynamics during head impact. SAE Technical Paper, No. 770922, 1977

[36] Trosseille, X., Tarriere, C., Lavaste, F., Guillon, F., and Domont, A. Development of a FEM of the human head according to a specific test protocol. *Proceedings of 36th Stapp Car Conference*, 1992: 235–253, Seattle, Washington (USA)

[37] Sabet, A. A., Christoforou, E., Zatlin, B., Genin, G. M., and Bayly, P. V. Deformation of the human brain induced by mild angular head acceleration. *J. Biomech.*, 2008, 41: 307–315.

[38] Kleiven, S. Influence of impact direction on the human head in prediction of subdural hematoma. *J. Neurotrauma*, 2003, 20(4):365–79.

[39] Gennarelli, T., Thibault, L., and Tomei, G. Directional dependence of axonal brain injury due to centroidal and non-centroidal acceleration. *Proceedings of the 31st Stapp Car Crash Conference*. 1987: 49–53.

[40] Smith, D. H., Nonaka, M., Miller, R., Leoni, M., Chen, X. H., Alsop, D., and Meaney, D. F. Immediate coma following inertial brain injury dependent on axonal damage in the brainstem. *J. Neurosurg.*,2000, 93(2): 315–322.

[41] Eucker, S. a, Smith, C., Ralston, J., Friess, S. H., and Margulies, S. S. Physiological and histopathological responses following closed rotational head injury depend on direction of head motion. *Exp. Neurol.*, 2011, 227(1): 79–88.

[42] Giordano, C., and Kleiven, S. Evaluation of Axonal Strain as a Predictor for Mild Traumatic Brain Injuries Using Finite Element Modeling. *Stapp Car Crash J.*, 2014, 58:29-61.

[43] Tsai, F., Teal, J., Itabashi, H., Huprich, J., Hieshima, G., and Segall, H. Computed tomography of posterior fossa trauma. *J Comput Assist Tomogr*, 1980, 4(3): 291–305.

[44] Margulies, S. S., Thibault, L. E., Gennarelli, T. A. Physical model simulations of brain injury in the primate. *J. Bomech*, 23(8), 823–36.

[45] Meaney, D. F., Smith, D. H., Sheriber, D. I., Bain, A. C., Miller, R. T., Ross, D. T., Gennarelli, T. A. Biomechanical analysis of experimental diffuse axonal injury. *J. Neurotrauma*, 1995, 12(4): 689–694.

[46] Ommaya, A., Yarnell, P., Hirsch, A., and Harris, E. Scaling of experimental data on cerebral concussion in sub-human primates to concussion threshold for man. SAE Technical Paper, No. 670906, 1967

[47] Stemper, B. D., Shah, A. S., Pintar, F. a, McCrea, M., Kurpad, S. N., Glavaski-Joksimovic, A., Olsen, C., and Budde, M. D. Head rotational acceleration characteristics influence behavioral and diffusion tensor imaging outcomes following concussion. *Ann. Biomed. Eng*., 2014, 43(5): 1071-88.

[48] Rowson, S., Duma, S. M., Beckwith, J. G., Chu, J. J., Greenwald, R. M., Crisco, J. J., Brolinson, P. G., Duhaime, A.-C., McAllister, T. W., and Maerlender, A. C. Rotational head kinematics in football impacts: an injury risk function for concussion. Ann. Biomed. Eng., 2012, 40(1):1–13.

[49] Rowson, S., and Duma, S. M. Brain Injury Prediction: Assessing the Combined Probability of Concussion Using Linear and Rotational Head Acceleration. Ann. Biomed. Eng., 2013, 41(5): 873–882.

[50] Zhang, L., Yang, K. H., and King, A. I. A Proposed Injury Threshold for Mild Traumatic Brain Injury. *J. Biomech. Eng.*, *J Biomech. Eng.*, 2004, 126(2): 226–236.

[51] Takhounts, E. G., Ridella, S. A., Tannous, R. E., Campbell, J. Q., Malone, D., Danelson, K., Stitzel, J., Rowson, S., and Duma, S. Investigation of Traumatic Brain Injuries Using the Next Generation of Simulated Injury Monitor (SIMon) Finite Element Head Model. *Stapp Car Crash J.*, 2008, 52:1–31.

[52] Cloots, R. J. H., van Dommelen, J. A. W., Kleiven, S., and Geers, M. G. D. Multi-scale mechanics of traumatic brain injury: predicting axonal strains from head loads. *Biomech. Model. Mechanobiol.*, 2012, 12(1): 137 – 150.

[53] Chatelin, S., Deck, C., Renard, F., Kremer, S., Heinrich, C., Armspach, J.-P., and Willinger, R. Computation of axonal elongation in head trauma finite element simulation. *J. Mech. Behav. Biomed. Mater.*, 2011, 4(8): 1905–19.

[54] Carlsen, R. W., and Daphalapurkar, N. P. The Importance of Structural Anisotropy in Computational Models of Traumatic Brain Injury. *Front. Neurol.*, 2015, 6:28.

[55] Broglio, S. P., Sosnoff, J. J., Shin, S., He, X., Alcaraz, C., and Zimmerman, J. Head impacts during high school football: a biomechanical assessment. *J. Athl. Train.*, 2009, 44(4): 342–9.

[56] Broglio, S. P., Surma, T., and Ashton-Miller, J. A. High school and collegiate football athlete concussions: a biomechanical review. *Ann. Biomed. Eng.*, 2012, 40(1): 37–46.